FINAL REPORT

Project Title: An Integrated Approach for Hydrogen Production and Storage in Complex Hydrides of Transitional Elements and Carbon-based Nanostructural materials

Project Period: July 1, 2006 to July 31, 2011

Recipient: University of Arkansas at Little Rock
Award Number: DE-FG36-06GO86054

Working Partners:

A. Bhattacharyya, A. S. Biris, M. K. Mazumder, T. Karabacak, Ganesh Kannarpady, R. Sharma,
Graduate Students: F. Cansizoglu, H. Ishihara, and M. Wolverton[1]
Undergraduate Students: D. Emanis and P. Girouard

Cost-Sharing Partners:

Arkansas Science and Technology Authority,
University of Arkansas at Little Rock

Contact: M. K. Mazumder, A. Bhattacharyya (Co-Principal Investigators)

M. K. Mazumder (Hydrogen Production)
mazumder@bu.edu, Phone: 617-353-9846

A. Bhattacharyya (Hydrogen Storage)
axbhattachar@ualr.edu, Phone: 501-569-8027

DOE Managers: DOE HQ Technology Manager: Ned Stetson
DOE Field Project Officer: Katie Randolph

[1] Dr.Mike Wolverton carried his research in Los Alamos National Laboratory, New Mexico in association with Dr.Luke Daemen. This work has benefited from the use of FDS at the Lujan Center at Los Alamos Neutron Science Center, funded by DOE Office of Basic Energy Sciences. Los Alamos National Laboratory is operated by Los Alamos National Security LLC under DOE Contract DE-AC52-06NA25396.

A. Provide an executive summary, which includes a discussion of I) how the research adds to the understanding of the area investigated; 2) the technical effectiveness and economic feasibility of the methods or techniques investigated or demonstrated; or 3) how the projectis otherwise of benefit to the public. The discussion should be a minimum of one paragraph and **written in terms understandable by an educated layman**.

Hydrogen Production

Hydrogen is an ideal renewable chemical fuel yet its production by splitting water with sunlight has been one of the most formidable challenges for the last several decades. There is an enormous potential for generating hydrogen directly from water by using sunlight. The process can provide inexhaustible and pollution free source of fuel replacing oil, gas and coal. Hydrogen can be utilized directly in internal combustion engines and can meet energy requirements for transportation as either a directly combusted chemical fuel or as component to hydrogen fuel cells. The goal of our project is to improve solar-to-hydrogen generation efficiency of the PhotoElectroChemical (PEC) conversion process by developing photoanodes with high absorption efficiency in the visible region of the solar radiation spectrum and to increase photo-corrosion resistance of the electrode for generating hydrogen from water. To meet this goal, we synthesized nanostructured heterogeneous semiconducting photoanodes with a higher light absorption efficiency compared to that of TiO_2 and used a corrosion protective layer of TiO_2. While the advantages of photoelectrochemical (PEC) production of hydrogen have not yet been realized, the recent developments show emergence of new nanostructural designs of photoanodes and choices of materials with significant gains in photoconversion efficiency.

Nanostructured Metal Hydrides for Hydrogen Storage

Development of solid state hydrogen storage materials is a critical challenge due to the difficulty in finding materials that have high gravimetric hydrogen density, stability over cycling, acceptable absorption-desorption temperatures, rates, and cost. Magnesium hydride, MgH_2, has the highest energy density (9 MJ/kg) among all reversible hydrides applicable for hydrogen storage. It combines a high gravimetric hydrogen capacity of 7.6 wt with the benefit of low-cost abundantly available magnesium. Hydrogenation/dehydrogenation is also fully reversible for Mg. However, Mg suffers from unfavorable kinetics and thermodynamics that dis not allow practical applications in the past.

Research on Mg has focused on reduction of absorption/desorption temperature which is around 300°C and to improve the re/de-hydrogenation kinetics. Catalyst additions and alloying have not been successful for desired properties so far. Nanostructuring of magnesium improves hydrogen absorption-desorption rates by benefiting from increased surface area of interaction and decreased diffusion lengths of hydrogen into/out-of Mg crystal. Thus both thermodynamics and kinetics of hydrogenation/dehydrogenation can be can be enhanced by nanostructuring Mg.

Glancing Angle Deposition (GLAD, a.k.a oblique-angle-deposition) has been an effective, easy to implement, and cost efficient technique to produce nanostructured coatings of a large variety of materials. It is an advanced version of physical vapor deposition (PVD) method and can be implemented through applying high vapor flux angles and/or substrate rotation on the sample surface in a sputtering, e-beam or thermal evaporation systems. GLAD can be implemented easily for large-scale production systems since it is already compatible with the current PVD infrastructure in the industry. Using GLAD metals are shown to have unique crystal properties such as non-preferential texture (i.e. crystal orientation) and single crystal structure. Magnesium is no exception for these and through the studies within this project, it has been shown that sputter-GLAD Mg nanorods have a single crystal structure with enhanced oxidation resistance properties. In addition, magnesium is an easy-to-evaporate material for PVD systems where very high growth rates can be achieved.

Mg depositions by thermal evaporation GLAD result in highly anisotropic nanotree structures composed of very thin (<20 nm) leaf morphologies. Nanotrees are composed of nanoleaves which can form groups that reach tens of microns in height and 1-2μm in lateral widths on the substrate. These structures are found to have oxidation resistance due to single crystal nature which further helps hydrogen diffusion. Studies on nanotrees showed enhanced hydrogen absorption characteristics of Mg. Hydrogen absorption was possible at temperatures as low as 100°C. Mg nanotrees absorbed as much as 3.9 wt% hydrogen when the temperature is increased from room temperature to 100 ^{o}C. As temperature is increased to 200, storage value reached up to about 4.4 wt%, and to a maximum storage value of about 7.3 wt% at 300 ^{o}C within ~10 minutes. In addition, significant desorption of hydrogen from magnesium hydride nanostructures occurred at temperatures ~200 ^{o}C. These enhancements are believed to be mainly through reduced size effects that help to alter thermodynamics of the system, decreased diffusion lengths, and crystal properties. The further enhancements is believed to be connected to uniform 3D hydride formation inside the Mg material, which could otherwise lead to a hydride shell on the outer surface and slowed hydrogen diffusion through this shell.

GLAD deposited Mg nanotrees offer the opportunity to investigate Mg structures with dimensions (<20 nm) that are not possible or is very elaborate with techniques such as high energy ball milling and thin film depositions. Thus it gives the opportunity to study nanostructuring effects on hydrogen absorption-desorption properties. These structures also open a window to study hydrogen diffusion in nanostructures, hydride formation and transformation, nucleation and growth. It is also easy to implement catalysts on the vast leaf surfaces and study catalyst effects on Mg metal and metal hydrides. Although it may end up different morphologies, by using co-deposition of various materials, GLAD Mg structures also allow studying alloys of magnesium. In this project we also demonstrated the fabrication of magnesium boride nanostructures using GLAD at room temperature, which was not achieved before. Such low temperature synthesis of Mg alloy nanostructures offer the possibility of developing new easy-to-fabricate materials for hydrogen storage.

Materials Research for Hydrogen Storage

Our contributions to hydrogen storage research include the following:

- We developed and successfully demonstrated an improved thermal model for volumetric hydrogen storage measurements [1]. In addition to increased accuracy versus empirical thermal models, this model allows for consecutive measurements at different temperatures without recalibration - which is not possible with empirical correction. This is useful for both cyclic sorption studies and temperature dependence studies.

- We synthesized previously untested materials for hydrogen storage properties. Materials tested include two titanium decorated conjugated polymers (Ti- polyaniline and Ti-polyphenylacetylene) inspired by theoretical studies [2]. Contrary to promising theoretical results, these Ti-decorated polymers were not found to be useful as hydrogen storage media [3].

- Group I and II borohydrides are among the highest hydrogen density of all potential storage media. However their thermal decomposition temperatures are too high, and reformation conditions too extreme. These difficulties are potentially overcome with catalysis. We were the first to test $LaNi_5$ alloy as a potential catalyst for $LiBH_4$ decomposition in both bulk and nanoparticle forms. A mild catalytic effect was observed, but it was deemed too insignificant to warrant further investigation.

- Nanoporous materials have been used to destabilize borohydrides allowing their decomposition at lower temperatures [4]. We demonstrated that transition metal doping of the nanoporous

scaffold can help with destabilization. Furthermore, our analyses indicate that surface interactions play a significant role in destabilization of two different tetraalkylammonium borohydride compounds [5].

Provide a comparison of the actual accomplishments with the goals and objectives of the project

Hydrogen Production

Goal:

Solar-to-hydrogen (STH) efficiency 10% by 2015 by developing photoanodes having efficient light absorption in the visible range and a long term corrosion resistance by reaching quantum yield of 30% at 600 nm for commercial scale H_2 production.

Accomplishments:

- Synthesized nanotubular TiO_2 photoanodes with stepped voltage anodization and surface modification of TiO_2 photoanodes with He plasma which minimized charge carrier traps and contaminants,
- Surface doping of the photoanode surface with nitrogen plasma followed by He plasma treatment, to form $TiO_{2-x}N_x$ at the surface thus leaving the bulk semiconductor for high electron conductivity and created oxygen vacancies at the surface for improved photocurrent density,
- Increased photocurrent density by more than 80% by plasma treatments and enhanced light absorption by 55% with modified nanotubular structure compared to the untreated TiO_2 photoanodes, and
- Synthesized of tandem heterostructured layered electrodes with lower bandgap layer (e.g. WO_3, $TiSi_2$,) behind a wide bandgap semiconductor (e.g. TiO_2) facing the electrolyte,
- Developed of self-cleaning solar concentrator for operating the PEC devices at irradiance level of 10 sun for enhancing hydrogen generation rate.

Nanostructured Metal Hydrides for Hydrogen Storage

We were able to accomplish original goals and objectives of our project where we demonstrated the enhanced effects of GLAD nanostructures on hydrogen storage properties. With the motive to investigate maximum hydrogen storage capacity, and adsorption/desorption kinetics in thin films and nanostructures of magnesium for hydrogen storage; we have conducted a study of Mg nanostructures deposited by GLAD. Their morphological and structural characterization was analyzed through SEM and XRD methods. Hydrogen absorption characteristics, thermodynamics and kinetics under different temperatures were studied using a new quartz crystal microbalance (QCM) system developed in this project. Hydrogen absorption studies were conducted under varying temperatures and compared to the behavior at constant temperatures. Desorption performances under constant temperatures were also measured. Our results showed superior hydrogen absorption and desorption properties for GLAD Mg nanostructures at low temperatures. In addition to the original goals of this project, per the suggestions on our previous reports by the DOE reviewers, we also investigated the fabrication and hydrogen storage properties of magnesium boride nanostructures using GLAD. We demonstrated the room temperature growth of magnesium boride coatings and their low pressure hydrogenation property, which have been challenging issues for this attractive material for hydrogen storage applications.

Materials Research for Hydrogen Storage

Goal: Increase of reversible hydrogen storage capacity in complex metal hydrides by developing new systems including hydride phases

Accomplishments - We synthesized new polymer materials predicted to be powerful hydrogen absorbers, and tested several new catalysis and destabilization techniques for borohydrides. The polymer materials were found to have no hydrogen absorbing properties. Some new catalytic effects for borohydrides were identified, but all are of insignificant potency to make borohydride based hydrogen storage viable. Our research did reveal a potential technique to improve the effectiveness of porous networks when used as scaffords for hydride complexes.

Goal: Investigate the effects of nanostructures on adsorption/desorption kinetics, and study surface oxidation properties.

Accomplishments - We are the first to analyze organic borohydrides in nanoporous silica networks as a model system. Our results are the first to reveal the importance of surface chemical interactions between the guest hydride complex and host network. Our results should encourage the use of metal doping and surface treatments to increase the effectiveness of porous networks used as scaffolds for hydride complexes.

Summarize project activities for the entire period of funding, including original hypotheses, approaches used, problems encountered and departure from planned methodology, and an assessment of their impact on the project results. Include, if applicable, facts, **figures**, analyses, and assumptions used during the life of the project to support the conclusions.

Hydrogen Production

Objectives

- Synthesize nanostructured $TiO_{2-x}N_x$ photoanodes and tandem heterostructured photoanodes with WO_3 and $TiSi_2$ to improve absorption of light in the visible spectrum in conjunction with TIO_2 film at the outer surface forming interface between the solid electrode and the liquid electrolyte,
- Improve photocatalytic properties of photoanodes by plasma treatments for (a) removing contaminants and unwanted surface states, (b) doping the photoanode surface with nitrogen to create oxygen vacancies and vacant acceptor states to enhance oxidation of water, (c) Optimizing surface structure of nanotubular electrodes for increasing photocurrent density,
- Design optical system with self-cleaning Fresnel-lens based solar concentrator to operate the PEC electrode at 10 sun irradiance, and
- Optimize surface structure of the layered electrodes for minimizing the charge carrier traps.

Approach

To address the problem related to the wide bandgap of TiO_2, one approach is to develop a hybrid nanostructured photoanode comprised of thin-film layers of semiconductors with lower bandgap (e.g. WO_3, $TiSi_2$,) behind a wide bandgap semiconductor (e.g. TiO_2) facing the electrolyte [6]. Similar photoanodes can be synthesized with nanotubular structures with outer layer of titanium dioxide (TiO_2) covering nanotubes of WO_3, CdS or $TiSi_2$. The low bandgap semiconductors have high efficiency in light absorption covering the visible solar spectrum while TiO_2 provides corrosion protection. The layered nanotubular electrodes can be arranged in a patterned array for trapping sunlight more effectively compared to the densely packed nanotubular structures, providing large illuminated area effective for

electrolysis. While the nanostructure greatly improves the reaction surface area and light absorption, the efficiency of the charge carrier transport across the interfaces and removal of charge carrier traps at the semiconductor-electrolyte interface need to be investigated for different heterostructures. including layered films, nanotubes and nanoparticles.

Interfacial charge carrier transfer phenomena govern the PEC based hydrogen generation process. Studies on the role of surface and interface states in the charge carrier transport and the necessity for matched lattice structure in using heterostructured semiconductors (such as TiO_2 and $TiSi_2$) have been reported in the literature [7], however, the chemical and physical control mechanisms for mitigating the losses due to the presence of charge carrier traps and minimization of photocorrosion of the electrodes are yet to be established.

Optimization of the optical system for illuminating photoanode at the desired irradiance level with solar concentrator is needed for obtaining maximum efficiency at a low cost. For collecting sunlight at the maximum level it is necessary to use a solar concentrator with self-cleaning properties to avoid loss of light transmission efficiency due to the deposition of dust. It is expected that large-scale PEC based hydrogen production facility will take place in semi-arid and desert locations where irradiance level is high but these places are often the dustiest locations. We have developed transparent electrodynamic screens that can be placed over a Fresnel lens, which can be used as a solar radiation concentrator for illuminating photoanodes using fiber optics.

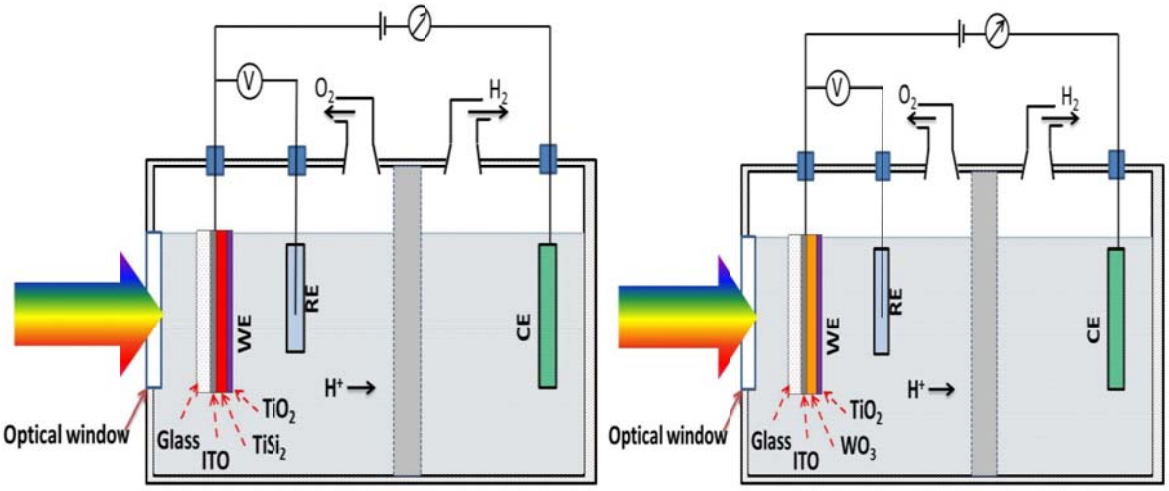

Figure 1. Experimental arrangement for photoelectrochemical generation of hydrogen using different photoanodes (a) hybrid $TiSi_2$ and TiO_2 electrode (left) and (b) hybrid WO_3 and $TiSi_2$ electrode (right). A Platinum counter electrode (CE) was used in both cases.

Experimental Studies and Results

Our experimental studies consisted of: (1) Synthesis nanotubular TiO_2 photoanodes by anodization of Ti foil followed by annealing under oxygen atmosphere, (2) Surface modification of TiO_2 photoanodes with He plasma for removing organic contaminants and charge carrier traps, (3) Surface doping of the photoanode surface with nitrogen plasma to form $TiO_{2-x}N_x$ and creating oxygen vacancies at the surface

thus leaving the bulk semiconductor pristine in its crystalline TiO_2 structure for high electron conductivity for improved photocurrent density [8], (4) Optimization of the structure of the nanotubes by varying anodization voltage for increasing light absorption, (5) Development of layered electrodes of WO_3, $TiSi_2$ and TiO_2, (6) Analysis of the photoanode structures using XPS, and (7) Evaluation of surface-modified nanostructured photoanodes for photoelectrochemical generation of hydrogen**.**

The test photoanodes prepared for evaluating the photoelectrolytic properties were annealed under both oxygen and nitrogen atmospheres achieve crystallization of TiO_2 in its anatase form. The photoelectrochemical apparatus used for measuring photocurrent density of the test photoanodes under dark and illuminated conditions consisted of (1) a Potentiostat/Galvanostat electrochemical instrument Model 283, (2) a Xenon lamp (30 mW/cm^2), (3) a 60 mm-diameter quarts optical window, and (4) a reference electrode (Ag/AgCl) placed close to the photoanode. The electrolyte used was 1M KOH (pH~14) + DI water solution. The experimental arrangements are shown in Fig. 1.

An electrodynamic screen was developed for operating solar concentrators using Fresnel lens with self-cleaning properties against deposition of dust on the sunlight collector surface [9]. A transparent electrodynamic screen can remove the dust layer in less than two minutes without any need for water or mechanical method for cleaning.

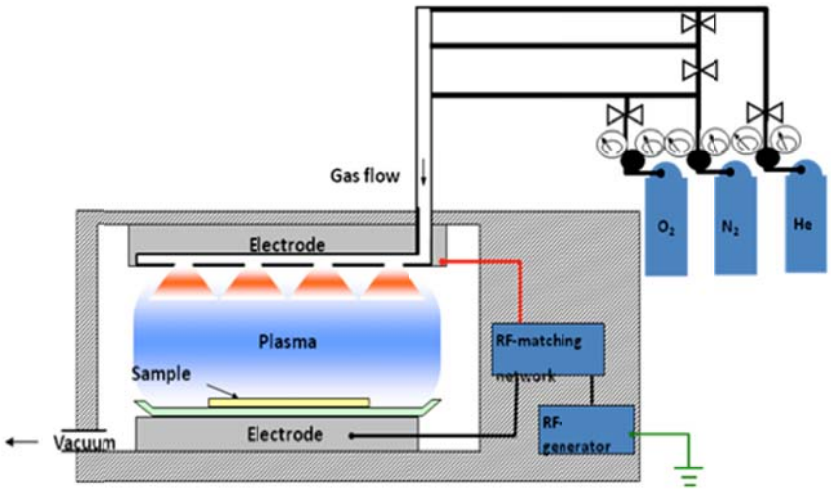

Fig. 2a. Schematic of low-pressure plasma reactor used for surface modification including He–plasma for surface cleaning and minimizing surface charge carrier traps followed by surface doping of with N-plasma to form $TiO_{2-x}N_x$ at the photoanode surface.

Results

XPS analysis indicated the incorporation of N in titania lattice structure of the photoanode surface. As shown in Fig. 2, the narrow scan N 1s spectrum is demonstrated at 400 and 396 eV, which has been ascribed to the presence of nitrogen in the lattice structure either as substitutional dopants for O, or as interstitial dopants in the TiO_2 crystal structure. Stepped-voltage anodization was used to synthesize

titania nanotubes of variable diameters. Photocurrent density vs bias voltage plotted for samples anodized at different voltages. Annealing of the photoanodes was optimized. Most significant improvement came from the nitrogen plasma treatment of titania photoanodes which resulted in 80% increase in photocurrent density.

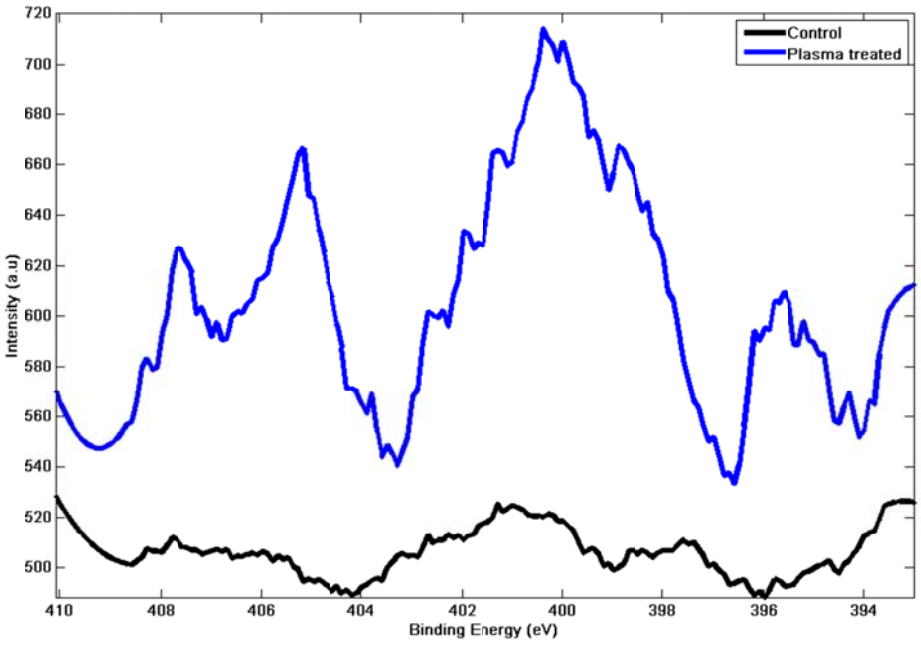

Fig. 2b. XPS spectrum (a) Control and (b) Nitrogen-Plasma treated $TiO_{2-x}N_x$ photoanodes

Plasma surface cleaning with helium plasma and surface doping by nitrogen plasma increased photocurrent density of titania nanotubular electrodes [8]. The results showed enhanced light absorption and increased photocurrent density by 55% [Fig. 3].

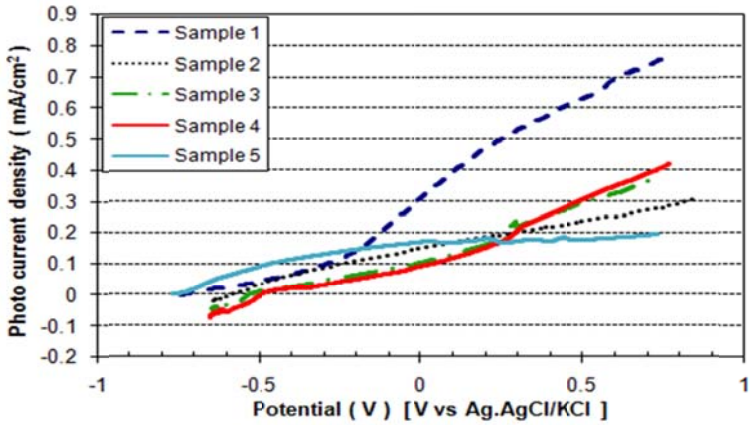

3(a) Photocurrent density vs. stepped voltage anodization of TiO2 nantubular electrodes; sample #1 was anodized at three steps: at 20 V for 40 min, next 40 V for 10 min, and finally 60 V for 10 min, Sample #2 was anodized in one step, 60 V for 60 min, sample #3 was anodized at 40 V for 60 min, and samples 4 and 5 were both anodized in one step at 20 V for 60 minutes.

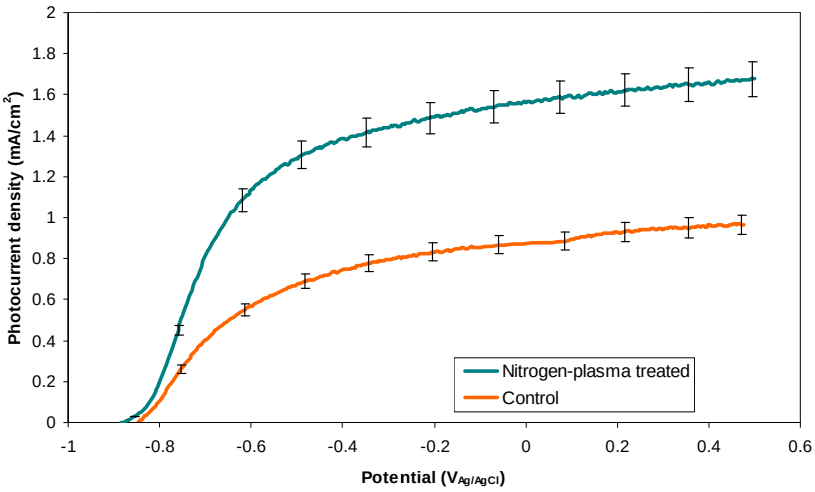

3(b) Photocurrent density measurements for control and nitrogen plasma treated titania photoanodes before and after N plasma treatment to form followed by He plasma cleaning. $TiO_{2-x}N_x$ was formed at the surface of TiO_2 nanotubes. Photocurrent density increased from 0.93 mA/cm^2 to 1.68 mA/cm^2 at a bias voltage of 0.2 V.

Fig. 3. Photocurrent density measurements for evaluating photoanodes synthesized under different conditions. The electrolyte used was 1M KOH (pH~14) + DI water solution. A Xe lamp was used to illuminate photoanodes at an irradiance level of 30 mW/cm^2

Several deposition processes for developing heterojunction $TiO_2/TiSi_2$ photoanodes have been studied; an e-beam deposition system has been used for depositing thin films of different photoanode

materials. An electrospray system has been designed for electrostatic coating of $TiSi_2$ particles with nanoparticles of TiO_2.

Further studies are needed to develop (1) Hybrid nanostructured photoanode comprised of thin-film layers of semiconductors with lower bandgap (e.g. WO_3, $TiSi_2$, CdS) behind a wide bandgap semiconductor (e.g. TiO_2) facing the electrolyte, (2) Patterned array of nanotubular electrodes for trapping sunlight more effectively compared to the densely packed nanotubular structures, providing large illuminated surface area effective for electrolysis, and (3) Encapsulated nanoparticles of core-shell design using narrow and wide bandgap materials.

Investigation of the charge carrier transport process across the interfaces and removal of charge carrier traps at the semiconductor-electrolyte interface by passivation of the dangling bonds for different heterostructures, including layered films, nanotubes and nanoparticles would provide further improvement of the photoanodes.

It is desired to develop methods for (1) optimizing the film thickness (in the nanometer to micrometer range, to improve tunneling and charge carrier transport), (2) matching the crystalline structures of the layered semiconductors and (3) measuring the photocurrent conversion efficiency (IPCE vs λ), corrosion resistance, and photo-generated carrier concentration decay rate (by using a rf-conductivity probe), and (4) investigate the use of self-cleaning solar concentrator for operating the PEC at an optimum irradiance level.

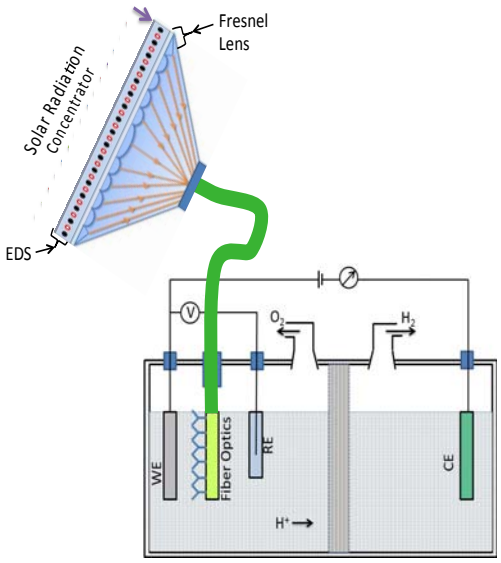

Fig 4a. Illumination of photoanode with self-cleaning solar concentrator at an irradiance level of 10 sun. A fiber optics based light coupling is used to allow illumination of the photoanode at the front surface of the electrode to minimize reflection loss at the outer glass optical window and at the back surface of the inner ITO coated glass substrate. An electrodynamic screen is used to remove dust deposited on the front surface of the Fresnel lens.

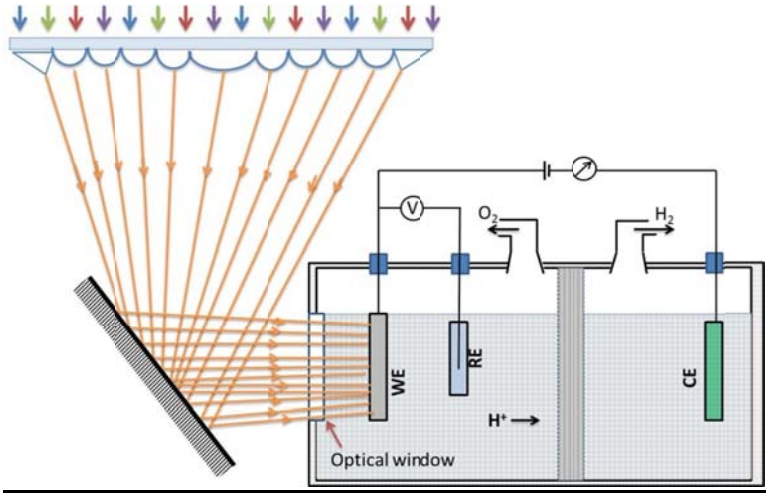

Fig 4b. Illumination of photoanode with self-cleaning solar concentrator at an irradiance level of 10 sun. A mirror is used is used to allow illumination of the photoanode at the back surface. This arrangement suffers from reflection losses at the outer glass window and the back surface of the inner ITO coated glass substrate. There is no fiber optic coupling loss in this arrangement.

Our experimental data show that deposition of fine atmospheric dust on solar collector with surface mass density of 4 g/m^2 can obscure sunlight by more than 40%. Design of a self-cleaning solar concentrator has been completed with mirrors and fiber optics for illuminating the photoanode surface at 10-sun level of irradiance is shown in Fig. 4.

Conclusions and Future Directions

Our experimental studies with plasma surface treatments with helium and nitrogen gas show a significant increase of $TiO_{2-x}N_x$ photoanode current density compared with the untreated surface of the electrodes. The nitrogen plasma treatment increased acceptor surface states and increased oxygen vacancies. Surface cleaning of the photoanode by low-temperature helium plasma treatment removed a major fraction of the contaminants (adsorbates) from the surface.

The present work reports the importance of systematic investigations of (1) the morphological structure of the nanotube arrays, (2) the plasma treatment process for surface doping of TiO_2 nanotubular photoanode with N for increasing oxygen vacancies and (3) optimization of the annealing process for crystallization of TiO_2 for improving photocatalytic generation of hydrogen from water. The test results show promising aspects of tuning several parameters involved in developing heterostructured photoanodes for PEC based hydrogen production. Development and design of self-cleaning solar concentrator for increasing solar irradiance at the photoanode surface is reported.

Nanostructured Metal Hydrides for Hydrogen Storage

During this DOE project, most of our initial focus was on the fabrication of magnesium nanostructures using thermal evaporation and sputter GLAD techniques and their hydrogen storage properties. Research conducted on thin film and nanostructured coatings required novel characterization

techniques for hydrogen absorption/desorption properties mainly due to very small amounts of material produced. Small weight loading specimens are not suitable for conventional hydrogen storage measurement techniques such as Sievert's apparatus. For this purpose we developed a new Quartz Crystal Microbalance (QCM) gas adsorption/desorption measurement technique. QCM method offers new opportunities to study thin film and nanostructures by analyzing mass changes due to absorption/desorption phenomenon at very precise amounts (i.e. 0.1 ng). A new QCM system that is capable of housing 2 samples and a residual gas analyzer unit (RGA) was designed to study hydrogen absorption on GLAD nanostructures (Fig. 5).

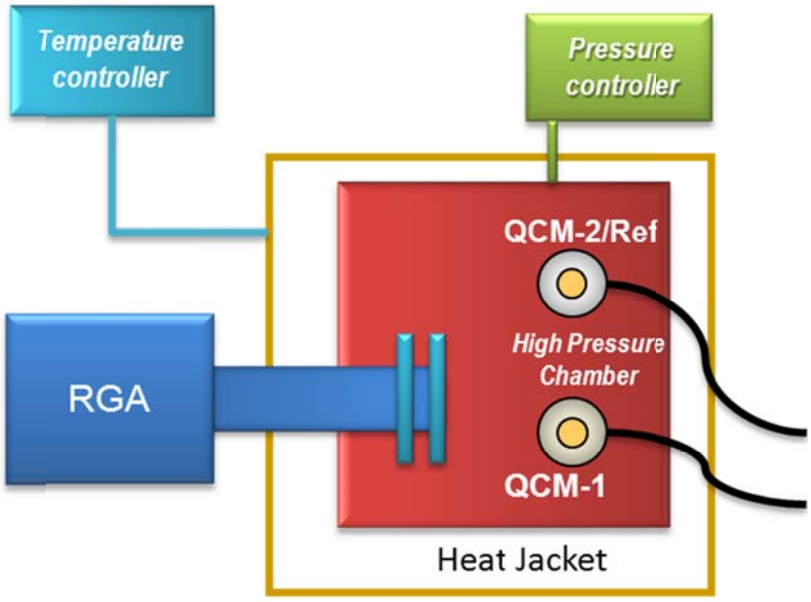

Figure 5: Quartz crystal microbalance (QCM) hydrogen storage measurement set-up

However, QCM crystals are sensitive to temperature, gas pressure, and surface roughness of the coating. This can make it difficult to analyze the dynamic change of hydrogen storage especially in experiments of variable temperatures. In order to eliminate these effects, we developed analytical models to convert experimental raw data to the corrected hydrogen storage values that allowed us to detailed kinetic studies.

In our experiments, nanotrees and conventional thin films of elemental Mg have been deposited directly onto the surface of gold coated unpolished quartz crystal substrates. The arrays of Mg nanotrees were about 15 µm long, 10 µm wide, and incorporated "nanoleaves" of about 20 nm in thickness and 1.2 µm in lateral width (Fig. 6).

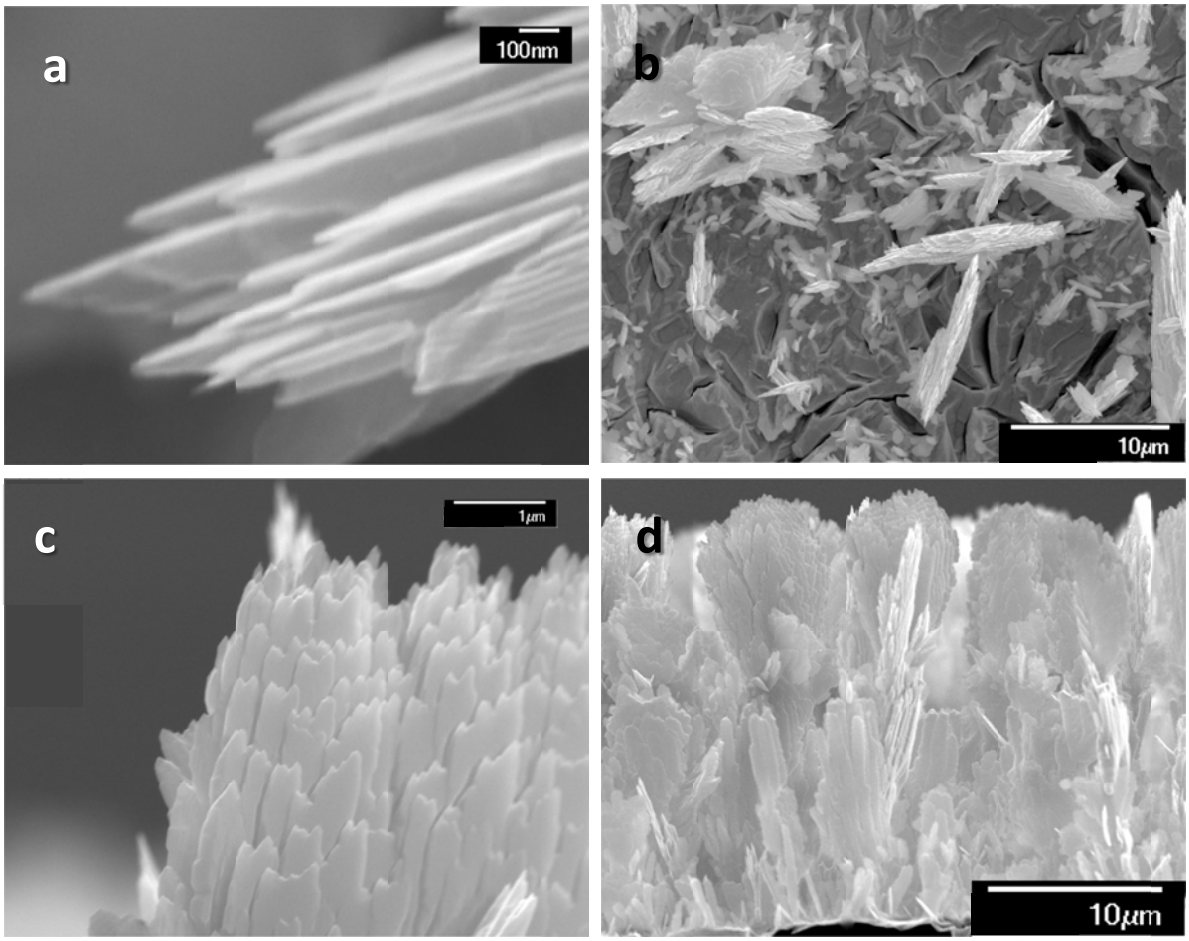

Figure 6: T**op-view (a-b) and cross-sectional (c-d) scanning electron microscopy (SEM) images of GLAD Mg nanotrees with stacks of nanoleaves grown on QCM substrates Cross-sectional (a-b) and are shown.**

Hydrogen storage properties of thin films and nanotrees were performed using our custom built QCM testing system (Fig. 5). Experiments were done at constant temperatures of 100 ^{o}C, 200 ^{o}C, and 300 ^{o}C at 30 bars of H_2 pressure. Another set was studied under increasing temperatures from room temperature up to 100 ^{o}C, 200 ^{o}C, and 300 ^{o}C to investigate the increasing temperature effect. Desorption tests were performed for constant temperature experiments by reducing the pressure to 10^{-3} mbars. QCM measurements revealed Mg nanotrees has enhanced absorption at temperatures as low as 100 ^{o}C, and even better when the variable temperature process is used. At 100 ^{o}C Mg nanotrees were able to absorb 1.47 wt% hydrogen, while it was only 0.30 wt% for Mg thin films (Fig. 7). However, Mg nanotrees' maximum storage capacity has reached 3.89 wt%, when the variable temperature procedure was used. At 200 ^{o}C, nanotrees and thin films of Mg absorbed 4.42 wt% and 1.05 wt%, respectively, while it reached about 6.10 wt% for nanotrees when gradual temperature increase was used. At 300^{o}C figures were 6.89 wt% vs 7.27 wt % at constant and variable temperature respectively for Mg nanotrees. The variable temperature process did not have a significant effect on the storage capacity values of Mg thin films compared to constant temperature experiments.

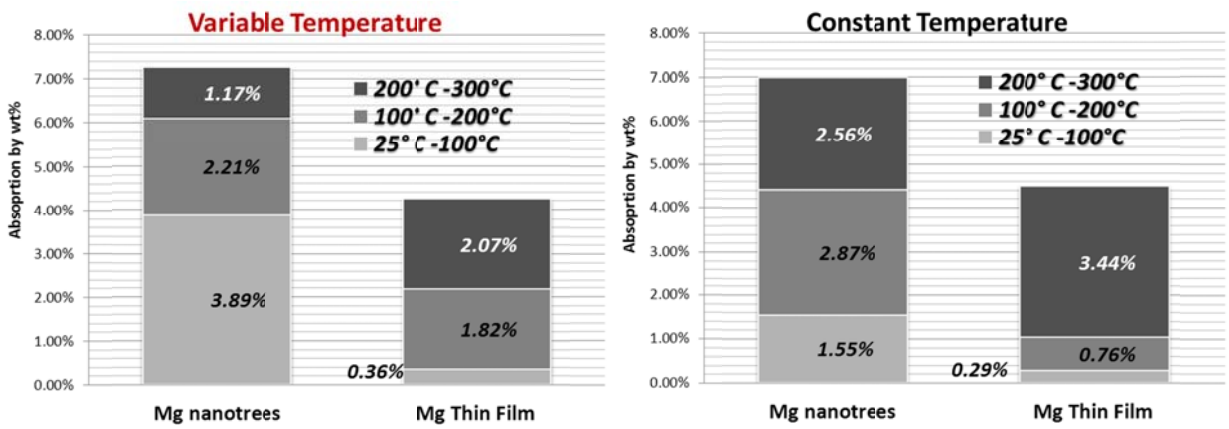

Figure 7: Hydrogen absorption wt%-temperature interval distribution for Mg nanotrees and thin films under variable and constant temperature QCM procedures at 30 bar H_2 pressure

Hydride formation at these temperatures was confirmed by X-ray diffraction (XRD) measurements. Scanning electron microscopy (SEM) analysis also showed that Mg nanotrees were able to accommodate the large volume expansion induced by hydrogenation, and structures did not suffer from agglomeration, cracking, or delamination from the substrate. Through Johnson-Mehl-Avrami-Kolmogorov (JMAK) analysis, we calculated the hydrogenation activation energy of Mg nanotrees for the constant temperature process as 87 kJ/mol, which was significantly lower than the 164 kJ/mol value of conventional Mg films. QCM oxidation tests performed under long term oxygen flow showed enhanced oxidation resistance of Mg nanotrees with no significant mass increase (less than 0.01 wt%). The significant enhancement in hydrogen absorption properties of GLAD Mg nanotree arrays is believed to originate from their very thin isolated nanoleaves with enhanced oxidation resistance. Further improvements in the maximum storage of Mg nanotrees in a variable temperature process can be attributed to the increase in the β-MgH_2 nucleation sites in Mg nanotrees.

Per the recommendations of the reviewers of previous reports on this DOE project, we also investigated the fabrication of magnesium boride nanostructures using GLAD sputter co-deposition of magnesium and boron and studied the hydrogenation properties at at 300 ^{o}C under H_2 pressure of 30 bar. XRD studies indicated magnesium borohydride peaks which are unusual at such levels of pressure and temperature. This study was also the first time a magnesium boride coating was achieved at a room temperature process, which is believed to offer several application opportunities.

Materials Research for Hydrogen Storage

1. Sieverts apparatus

A high temperature, high pressure volumetric gas titration system (Sieverts apparatus) was designed and fabricated by us. This instrument was designed to incorporate a novel temperature differential model to account for thermal gradients in the reactor and attached conduits. During construction we encountered some difficulty in the form of a faulty valve which, unknown to us, contained a material permeable to hydrogen as an internal seal. Locating and removing this faulty component proved time consuming and extended the construction time more than anticipated. After proper function of all components was verified, a careful systematic characterization was performed and the temperature differential model was validated with simple gas transfer and temperature adjustment experiments. We then performed a short thermodynamic

and cyclic sorption study on the well known hydrogen absorbing alloy $LaNi_5$ for further proof of the instrument. Further details of the design and verification of our Sieverts apparatus are published elsewhere [1].

Results and impact - The thermal model we developed provides an improved alternative for approaching design and measurement in modern Sieverts apparatuses.

2. $LiBH_4$ catalyzed by $LaNi_5$

Following the construction of our Sieverts apparatus, we began work investigating catalysis of hydride complexes motivated by their high hydrogen content (and likewise the high target capacities of the Freedom Car program). We returned to $LaNi_5$ investigating it this time as a potential *catalytic additive* for hydrogen sorption in hydride complexes. Our hypothesis was that the interface of the complex hydride with a metal that has a high affinity for hydrogen (such as $LaNi_5$) would facilitate catalytic activity by providing an intermediate step, with intermediate binding energy, during absorption or desorption.

Preliminary work began on $NaAlH_4$ ground with small quantities of activated and cycled $LaNi_5$. We observed a reduction in decomposition temperature and increase in rate of hydrogen release, but did not carefully characterize the system with knowledge that $NaAlH_4$ had been down selected and would not be able to meet systematic capacity requirements. We thus moved on to a testing for catalytic effects in the desorption of a complex hydride with greater hydrogen content, $LiBH_4$. The primary decomposition of $LiBH_4$ typically begins around 425°C; whereas we reliably recorded some hydrogen release at ~300°C when ground with activated $LaNi_5$. However the quantity of hydrogen released at this temperature was very small. In an effort to make this effect more pronounced, nanoparticles of $LiBH_4$ were produced by combustion synthesis (Cs-$LaNi_5$) similar to the method in [10]. It was found that a small portion (~5% of the total $LiBH_4$ hydrogen content) was released quickly at 235°C when ground with $LaNi_5$ as seen in Figure 8.

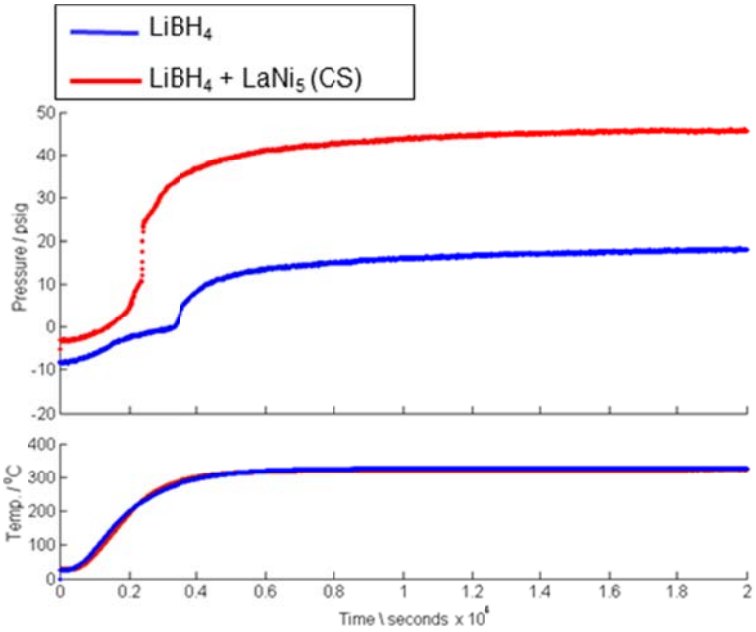

Figure 8 Heating of $LiBH_4$ and $LiBH_4$/CS-$LaNi_5$

While the addition of $LaNi_5$ nanoparticles clearly causes a strong reduction in decomposition temperature and increase in rate of hydrogen release, the desorption reaction reliably halts after 5-10% of the total hydrogen content of the $LiBH_4$ has been released.

A likely explanation is that $LaNi_5$ nanoparticles have a catalytic effect on $LiBH_4$ decomposition, but access to the $LaNi_5$ surface is obscured during $LiBH_4$ decomposition by the decomposition byproducts. An adequate solution to this problem was not determined.

Results and impact - it is possible that $LaNi_5$ can be used to catalyze $LiBH_4$ if a reaction method can be determined that prevents the surface of the metallic hydride from being obscured. Otherwise $LaNi_5$ is of little utility as a catalytic additive.

3. $LiBH_4$ / $Ca(BH_4)_2$ coupled reaction

We explored the possibility of a more thermodynamically favorable decomposition reaction for group 1 and 2 borohydrides by coupled decomposition. Specifically, the following reaction was predicted to be thermodynamically favorable by Ozolins et al. [11]:

$$5Ca(BH_4)_2 + 2LiBH_4 \rightarrow Li_2B_{12}H_{12} + 5CaH_2 + 13H_2 \qquad \text{(6.7\% mass } H_2 \text{ released)}$$

While this reaction releases less hydrogen than the decomposition of either $LiBH_4$ or $Ca(BH_4)_2$ alone, the theoretically predicted enthalpy change of the reaction (37 kJ mol^{-1}) is less endothermic than the decomposition of either neat borohydride [11]. There was also the possibility of a subsequent reaction between the produced $Li_2B_{12}H_{12}$ and CaH_2.

We tested the above decomposition reaction by heating ballmilled mixtures of $LiBH_4$ and $Ca(BH_4)_2$ (at a stoichiometric ratio of 2:5 as implied above) under inert atmosphere. This time thermogravimetric measurements were used to evaluate hydrogen release. A measured a mass loss (0.5 - 0.7%) with an onset around 215°C was repeatable accompanied by a new endothermic peak in the DSC signature. Neither of these features occurs during the heating of either neat $LiBH_4$ or $Ca(BH_4)_2$. Additionally, the endothermic peak which typically accompanies $LiBH_4$ melting was absent from all runs. DSC/TGA data from such a measurement is shown in Figure 9.

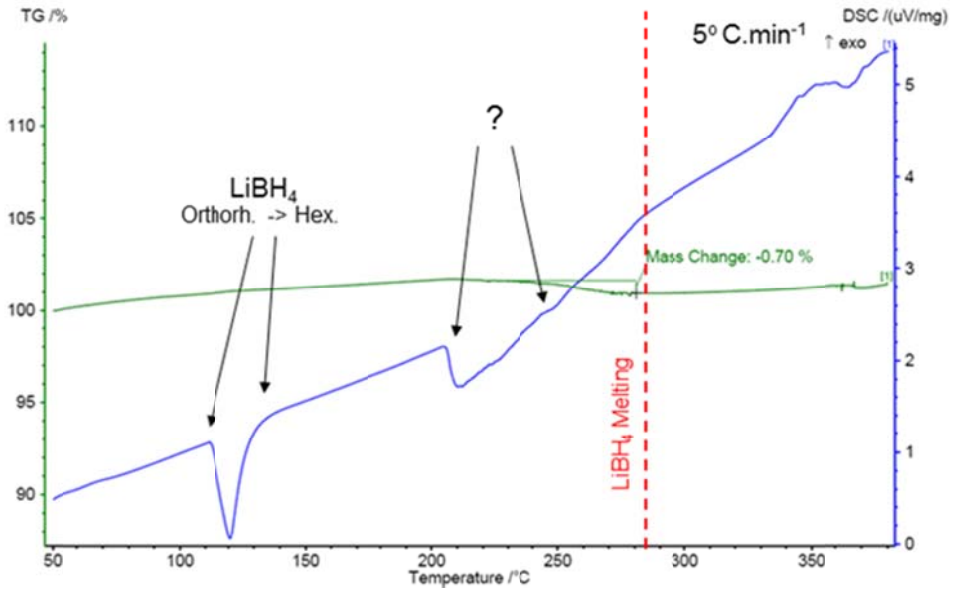

Figure 9 DSC/TGA of a ballmilled mixture of $LiBH_4/Ca(BH_4)_2$. The second endothermic peak of the DSC was previously identified (in error) as $LiBH_4$ melting. It is more likely attributable to a decomposition reaction from destabilization effects.

This thermal analysis implies some thermodynamic destabilization is occurring with the mixture of $LiBH_4$ and $Ca(BH_4)_2$. However, only a small fraction of the expected mass loss was obtained, indicating that the reaction does not go to completion. The FTIR spectrum of the residual material from heating the $LiBH_4/Ca(BH_4)_2$ mixture did not show any evidence of the $[B_{12}H_{12}]^{-2}$ anion, as would be expected from the theoretical predictions in reference [11]. A spectrum of the residual along with a sample $[B_{12}H_{12}]^{-2}$ containing salt can be seen in Figure 10.

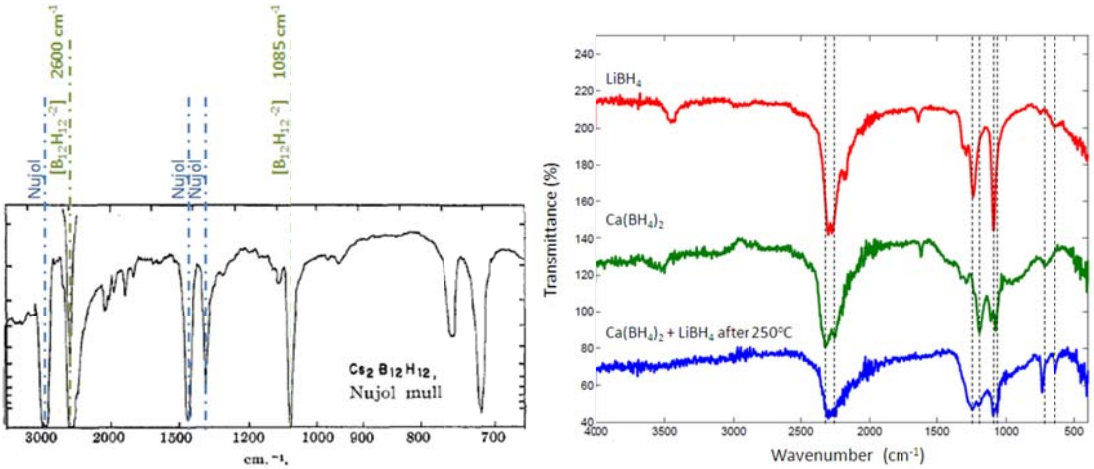

Figure 10 Infrared spectra. (left) Data for the $Cs_2B_{12}H_{12}$ in nujol taken from Muetterties et. al. [12] as an example of an alkali salt containing $[B_{12}H_{12}]^{-2}$ anion. (right) $Ca(BH_4)_2$ + $LiBH_4$ ballmilled mixture after heating to 250°C with reference spectra of $LiBH_4$ and $Ca(BH_4)_2$. There is no evidence of $[B_{12}H_{12}]^{-2}$ species.

Subsequent research of the coupled $LiBH_4/Ca(BH_4)_2$ system was halted due to the tendency of the decomposition reaction not to proceed to completion, and significant deviation from theoretical predictions.

Results and impact - We have observed a destabilization effect caused by mechanical mixing of $LiBH_4$ and $Ca(BH_4)_2$. However, it is unclear if the reaction proceeds as Ozolins et. al. predict [11]. The reaction temperature, hydrogen yield and kinetics of the observed $LiBH_4/Ca(BH_4)_2$ decomposition reaction are still insufficiently improved to be directly usable in hydrogen storage.

4. Ti-decorated polymers

A published study based on the theoretical calculations of Lee et. al. indicated that a series of conjugated polymers with periodically bound transition metals might function effectively as hydrogen storage media [2]. Their calculations indicated that metal sites on certain polymers can facilitate binding to multiple H_2 molecules (per site) with sufficient energy to allow adsorption at room temperature and a pressure of 1 bar H_2. Among the metal decorated polymers surveyed by Lee et al.[2], the Ti-decorated polymers exhibited the most favorable binding energies and number of adsorbed H_2 molecules per site.

Inspired by this study, we attempted the synthesis of two titanium decorated polymers by reaction of bulk polymer powder with titanium nanoparticles. Titanium decorated polyaniline (Ti-PANI) was included in two different bonding configurations among the calcuations of Lee et al. [11].

Titanium decorated polyphenylacetylene (Ti-PPA) was not explicitly included in reference [11], but was chosen for its chemical similarity to titanium decorated polyacetylene, which was included in reference [11].

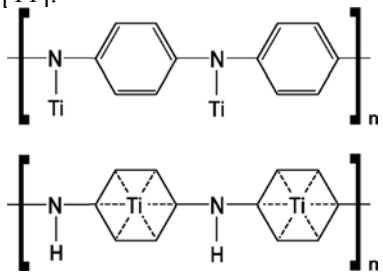

Figure 11 Bonding schemes for titanium decorated polyaniline developed from Fig.1(e) and (f) of reference [11].

For the Ti-PANI sample, we have reasonable spectroscopic evidence that we achieved the top binding scheme in Figure 11 calculated by Lee et al. We were not able to directly verify the Ti-N binding, but the titanium particles were consumed in the synthesis, and FTIR analysis indicated the stretching mode of the N-H bond had disappeared from the emeradine base polyaniline. Additionally the remainder of the resulting IR spectrum was consistent with our own *ab-initio* calculated vibrational frequencies of titanium substituted diphenylamine (a reasonable model system for the top chain of Figure 11). For more details of the synthesis and spectral analysis see [3]. Our analyses are consistent with achievement of the Ti-N type bonding scheme. The IR analysis also revealed that our Ti-polymer samples did contain some residual mineral oil from the synthesis procedure.

Neither of these polymers displayed any hydrogen sorption properties of any kind. Hydrogen sorption measurements were conducted on a 1 g sample of the Ti-PANI. Initial conditions for absorption were room temperature (25^{o}C), 30 bar H_2 as suggested by Lee et al. [11]. Gas was administered from a reference volume by dosing so that fast absorption could be accounted for. These conditions were maintained for two hours with no evidence of absorption, followed by an increase in H_2 pressure to 100 bar by further dosing (so that all gas is accounted for). These conditions were maintained for 12 hours with no evidence of H_2 absorption. Hydrogen was then vented from the Ti-PANI, which was then heated under vacuum to 200^{o}C to test for desorption. Unsurprisingly, no gas emission of any kind was measured. Additional heat treatments at 200^{o}C, 100 bar H_2 were subsequently performed on the Ti-PANI sample followed by further absorption testing at room temperature, 100 bar H_2. No hydrogen sorption activity of any kind was measured with the Ti-PANI sample. An identical series of sorption tests were performed on a 0.5g sample of Ti-PPA. The was no measurable absorption or emission of hydrogen by this material.

Results and impact - We attempted to synthesize two titanium decorated polymers which were predicted to absorb large quantities of hydrogen at room temperature [11]. While direct evidence of the metal-polymer bonds was not observed, analyses are consistent with the formation of the predicted metal decoration sites. No hydrogen sorption activity of any kind was observed for either titanium nanoparticle treated polymer, Ti-PANI and Ti-PPA. The reason for the lack of adsorption is somewhat ambiguous, but is likely due to the blockage of these sites by clustering or coverage by residual mineral oil.

5. R_4NBH_4 in MCM-48

It has been demonstrated that $LiBH_4$ is thermodynamically destabilized (catalyzed) by inclusion in mesoporous carbon resulting in a lower temperature for decomposition and reformation [4]. In an attempt to improve upon these effects we imitated a study of borohydride decomposition in mesoporous silica, originally intending to use $LiBH_4$ as the borohydride. MCM-48, a mesoporous silica, was selected as the host network because it can be synthesized as a repeating pore network (advantageous for analysis) and it is more easily adaptable by doping and surface chemical treatment than porous carbon networks.

For this study, $LiBH_4$ was to be deposited within the MCM-48 from solution by a volatile solvent which would be removed under vacuum. Analysis indicated that $LiBH_4$ was not entering the pore network and merely depositing on the surface of MCM-48 particles. Borohydrides with an organic cation (R_4NBH_4, R=CH_4, C_2H_5) were substituted for $LiBH_4$ as loading was easier to achieve with a wider selection of compatible solvents. Deep pore infiltration and relatively homogeneous loading were verified by complementary XRD, BET and FTIR analyses (for more details see reference [5])

The thermal decomposition of both Me_4NBH_4 and Et_4NBH_4 occurs at a substantially lower temperature inside the pores of MCM-48. A reduction in thermolysis onset temperature of about 100°C was seen in Et_4NBH_4, and a 120°C reduction in thermolysis onset for Me_4NBH_4. TGA data comparing decomposition of the bulk borohydrides and MCM-48 loaded materials can be seen in Figure 12.

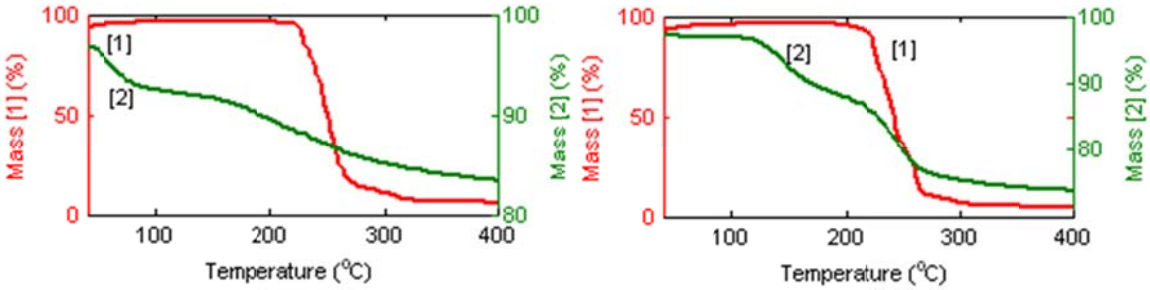

Figure 12 **(left)** TGA 5K/min. 1) Bulk Me_4NBH_4. 2) Methyl MCM-48 loaded with Me_4NBH_4. **(right)** TGA 5K/min. 1) Bulk Et_4NBH_4. 2) Methyl MCM-48 loaded with Et_4NBH_4.

Doping of the MCM-48 with Nickel furthered the destabilization effect. The nickel doped material was slightly less effective after a surface methylation treatment. TGA data showing the improved catalysis of Me_4NBH_4 from nickel doping can be seen in Figure 13.

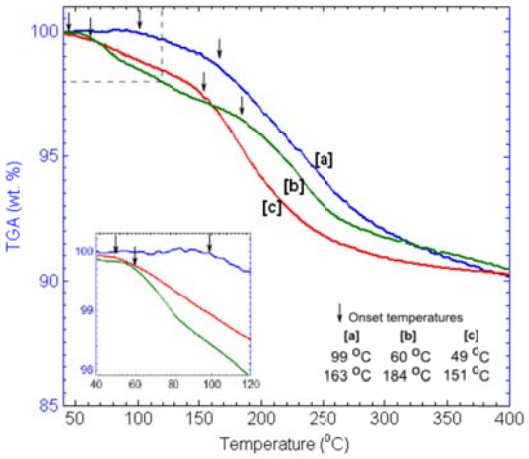

Figure 13 TGA 5K/min. **a)** methyl MCM-48 loaded with Me_4NBH_4 **b)** Methyl Ni-doped MCM-48 loaded with Me_4NBH_4. **c)** Ni-doped MCM-48 loaded with Me_4NBH_4.

Due to the potency of the demonstrated effects, analysis on this system was deepened to include studies of the vibrational spectrum. Our hope was to be able to identify characteristics of the destabilization process that would guide us in improving catalysis. Inelastic neutron scattering was employed allowing measurement of the vibrational spectrum of R_4NBH_4 deep within the MCM-48 porous silica network.

INS vibrational spectra were obtained for both Me_4NBH_4 and Et_4NBH_4 in bulk and adsorbed states as well as at various stages of thermal decomposition. Among our findings two were most significant:

1) Borohydrides adsorb and line the pore walls. This is apparent from significant low frequency perturbations in the vibrational spectrum after loading (see [5] for more details). Such perturbations can be seen for Me_4NBH_4 in Figure 14.
2) Surface sites play an active role in decomposition. This was apparent from the appearance of new vibrational modes during partial decomposition, as well as the variance in surface compounds left behind after decomposition, which varied depending upon the cation (Et_4N vs Me_4N), and presence of nickel sites. A comparison of Me_4NBH_4 spectra for adsorption in plain and nickel-doped MCM-48 can be seen in Figure 15 along with the spectra of the respective surface residual compounds resulting from decomposition.

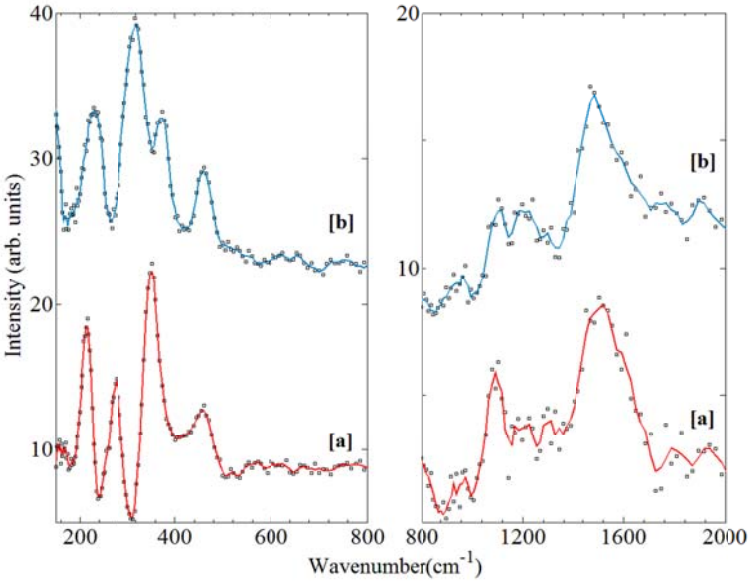

Figure 14 INS vibrational spectra. **a)** Bulk Me_4NBH_4. **b)** Me_4NBH_4 adsorbed on MCM-48.

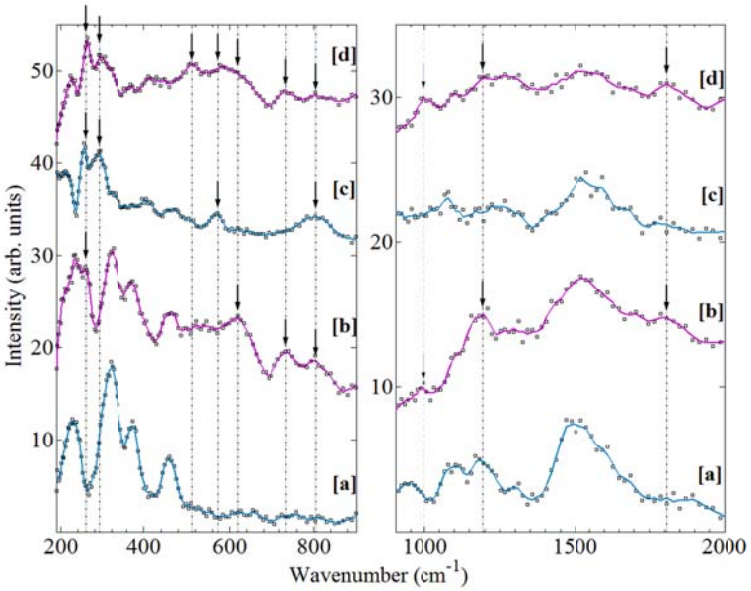

Figure 15 INS vibrational spectra Me_4NBH_4 adsorbed on plain MCM-48 vs. Me_4NBH_4 adsorbed on Ni-MCM-48 and result of thermolysis of each. **a)** Me_4NBH_4 adsorbed on methylated plain MCM-48 **b)** Me_4NBH_4 adsorbed on methylated Ni-MCM-48 **c)** sample from a. after 30 min. each at 100 ^oC, 200^oC and 300^oC **d)** sample from b. after 270^oC, 2hr.

Results and impact - This study as important implications for researchers pursuing porous networks in the catalysis / destabilization of borohydrides. The surface chemistry of the porous host, and role of the pore wall in destabilization are both of much greater significance than previously thought.
We hope these results encourage the use of metal doping and surface treatments in porous networks used as scaffolds for hydride complexes.

A> Identify products developed under the award and technology transfer activities, such as:

a. Publications

1. R. Sharma, P. P. Das, V. Mahajan, J. Bock, S. Trigwell, A. S. Biris, M. K. Mazumder, M. Misra, "Enhancement of Photoelectrochemical Conversion Efficiency of Nanotubular TiO_2 Photoanodes using Nitrogen Plasma Assisted Surface Modification," *Nanotechnology*, Vol. 20, 2009, 075704.

2. Mazumder, M. K., Biris, A. S., Johnson, C. E., Yurteri, C. Y., Sims, R. A., Sharma, , K. Pruessner, S. Trigwell and. Clements, *Particles on Surfaces 9: Detection, Adhesion and Removal, Brill Publisher,, 2006, pp.1-29. ISBN 90 6764 435 8.*

3. Cansizoglu, M. F and Karabacak T., "Hydrogen Storage Properties of Magnesium Nanotrees Investigated by a Quartz Crystal Microbalance System," (2011) (Submitted)

4. Bayca, S. U., Cansizoglu M. F., T. Karabacak et al.. "Enhanced oxidation resistance of magnesium nanorods grown by glancing angle deposition." International Journal of Hydrogen Energy 36(10): 5998-6004 (2011).

5. Cansizoglu, M.F. and T. Karabacak. "Enhanced Hydrogen Storage Properties of Magnesium Nanotrees with Nanoleaves". MRS Proceedings, 1216 : 1216-W05-03 Materials Research Society 2010 DOI: 10.1557/PROC-1216-W05-03 (2009).

6. Cansizoglu M. F., Watanabe F., Wang P.-I., and Karabacak T., "Evolution of crystal orientation in obliquely deposited magnesium nanostructures for hydrogen storage applications", MRS Proceeding, 1042: 1042-S04-06 Materials Research Society 2010 DOI:10.1557/PROC-1042-S04-06 (2007).

7. "Hydrogen Storage Properties of Magnesium Nanotrees by Glancing Angle Deposition" Cansizoglu M. F., and Karabacak T., AVS 57th international Symposium, Albuquerque, NM, October 17-22, 2010.

8. "Hydrogen Storage Properties of Magnesium Nanotrees by Glancing Angle Deposition" Cansizoglu M. F., and Karabacak T., APS March Meeting 2011, Dallas, TX, March 21–25, 2011.

9. A. Bhattacharya, T. Karabacak, F. Cansizoglu, M. Wolverton, "An Integrated Approach of Hydrogen Storage in Complex Hydrides of Transitional Elements", Annual DOE Review Meeting, Washington, DC, May 20, 2009.

10. M. J. Wolverton, G. K. Kannarpady, A. Bhattacharyya "A temperature differential model-based Sieverts apparatus" *Instrumentation Sci. & Tech.* **39,**2 (2011) 173-197.

11. M. J. Wolverton, G. K. Kannarpady, A. Bhattacharyya, D. P. Emanis "Investigation of Titanium Decorated Polyaniline and Polyphyenylacetylene for use as Hydrogen Storage Materials" *Global J. of Inorg. Chem.* **2,**1 (2011) 12-17.

12. M. J. Wolverton, L. L. Daemen, M. A. Hartl "Quaternary Ammonium Borohydride Adsorption in Mesoporous Silicate MCM-48." *Mater. Res. Soc. Symp. Proc.* **1262** (2010) paper no. 1262-W03-03.

c. Networks or collaborations fostered;

Nanostructured Metal Hydrides for Hydrogen Storage

Materials Research for Hydrogen Storage

- The experimental data collected for the investigation of borohydride destabilization by nanoporous silica was collected at the Los Alamos Neutron Science Center (LANSCE) at Los Alamos National Laboratory (LANL). For this portion of the project we wish to acknowledge our benefit from the use of the Lujan Center at LANSCE.

d. Technologies/Techniques;

Nanostructured Metal Hydrides for Hydrogen Storage

1. Quartz Crystal Microbalance (QCM) gas absorption/desorption system for the hydrogen storage measurements for thin films, nanostructures, and other types of low-weight loading coatings.

Materials Research for Hydrogen Storage

-We developed a differential thermal model for the reactor component of volumetric measurement systems [1]. This model has improved accuracy versus empirical thermal models and additionally allows for consecutive measurements at different temperatures without recalibration - which is not possible with empirical correction. This is useful for both cyclic sorption studies and temperature dependence studies.

f. Other products, such as data or databases, physical collections, audio or video, software or netware, models, educational aid or curricula, instruments or equipment.

Nanostructured Metal Hydrides for Hydrogen Storage

Materials Research for Hydrogen Storage

-We fabricated a custom computer automated Sieverts apparatus based on the aforementioned temperature differential model [1].

References:

1. M. J. Wolverton, G. K. Kannarpady, A. Bhattacharyya "A temperature differential model-based Sieverts apparatus" *Instrumentation Sci. & Tech.* **39,**2 (2011) 173-197

2. Lee, H.; Choi, W. I. and Ihm J. "Combinatorial Search for Optimal Hydrogen-Storage Nanomaterials Based on Polymers" *Phys. Rev. Letters* **2006,** 97, 056104.

3.M. J. Wolverton, G. K. Kannarpady, A. Bhattacharyya, D. P. Emanis "Investigation of Titanium Decorated Polyaniline and Polyphyenylacetylene for use as Hydrogen Storage Materials" *Global J. of Inorg. Chem.* **2,**1 (2011) 12-17

4. Fang, Z.; Wang P.; Rufford, T.; Kang, X.; Lu, G. and Cheng, H. "Kinetic- and thermodynamic-based improvements of lithium borohydride incorporated into activated carbon" *Acta Mat.* **2008**, 56, 6257.

5. M. J. Wolverton, L. L. Daemen, M. A. Hartl "Quaternary Ammonium Borohydride Adsorption in Mesoporous Silicate MCM-48." *Mater. Res. Soc. Symp. Proc.* **1262** (2010) paper no. 1262-W03-03

6. Zhang, J. Z., *MRS Bulletin, Material Research Society, vol. **36**, Jan 2011, 48 – 55.*

7.Hernandez-Alonso, M. D., Fresno, F., Surez, S.,and Coronado, J. M., *Energy Environ. Sci, The Royal Soc. of Chemistry,* 2009, 2, 1231 – 1257

8.R. Sharma, P. P. Das, V. Mahajan, J. Bock, S. Trigwell, A. S. Biris, M. K. Mazumder, M. Misra, "Enhancement of Photoelectrochemical Conversion Efficiency of Nanotubular TiO_2 Photoanodes using Nitrogen Plasma Assisted Surface Modification," *Nanotechnology*, Vol. 20, 2009, 075704.

9.Yu J C, Lin J, Lo D and Lam S K 2000 *Langmuir* **16** 7304

10. Xiao, Y.; Liu, Y; Yuan, D.; Zhang, J.; Me, Y. Synthesis of rod-shaped $LaNi_5$ alloy via solid reduction method *Materials Letters,* **2006,** 60, 2558–256.

11. Ozolins, V.; Majzoub, E. H.; Wolverton, C. "First-Principles Prediction of Thermodynamically Reversible Hydrogen Storage Reactions in the Li-Mg-Ca-B-H System" *J. Am. Chem. Soc.* **2009***, 131*, 230.

12. Muetterties, E. L.; Balthis, J. H.; Chia Y. T.; Knoth, W. H. and Miller H. C. " Chemistry of Boranes .8. Salts + Acids of $B_{10}H_{10}^{-2}$ + $B_{12}H_{12}^{-2}$" *Inorg. Chem.,* **1964,** 3 (3), 444.